ANGLES BETWEEN CRACKS DEVELOPED AT PRIMARY SHRINKAGE OF FINEGRAINED SOIL MATERIAL

K.H. Hartge[1], J. Bachmann[2]

[1]Habichthorst 9, D-30823 Garbsen, Germany,
[2]Institut für Bodenkunde, Herrenhäuser str. 2, D-30419 Hannover, Germany
E-mail: bachmann@mbox.ifbk.uni-hannover.de

A b s t r a c t. Angles which are formed between two cracks during primary shrinking were investigated at three open air sites and three laboratory experiments from literature. The objective was to determine the proportion between orthogonal angles (OA) and non orthogonal angles (NOA) in order to assess relative frequency of tensile and shearing cracks. Measurements were performed on photos and on copies from literature figures with a size of 30x21 cm (DIN A4) with a plane goniometer. The accuracy of reading was between ±2 and ±4° depending on the quality of magnification of figures and photos and the geometric form of the cracks. OA were observed in all cases. They were assumed to be tension-shrinkage-cracks. NOA were also observed in all cases. They were considered to be shear cracks. The means of these shear angles were calculated separately for those >90° and those <90°. The sum of means of both of these groups was close to 180°. Angles of internal friction (AIF) at the moment of cracking calculated from these means showed the lowest friction at cracking in the frozen soil, highest in the airdried laboratory samples and in the soil from the arid area. All the calculated AIF were in the order of magnitude that was obtained by direct shearing in an earlier investigation.

K e y w o r d s: shrinkage, cracking patterns

INTRODUCTION

If fine grained soil material dries the first time after being freshly sedimented from aquaeous suspension or from remolding, cracks will form. Under these conditions the volume will be subject first to normal shrinkage. For the various patterns of cracks which are observed during this contraction process the retreat of water menisci is generally considered to be the only cause of primary cracking.

Investigations of cracking patterns which are given in literature are directed to different details, i.e., distance of cracks [5], continuity of cracks [2,13], combination of clay-minerals [1], icrocracking due to water supply [3], general distribution of directions [12,13], crack propagation [13], causes of heterogeneity [11], geometrical forms of aggregates [8]. The crack in clay samples subject to uniaxial load develops secondary cracks that extended from its tips in a direction that deviates from the original crack. The angle of propagation of the secondary cracks is water content dependent [13]. To this end, angles which are formed between two connected cracks were not taken into consideration yet. It was therefore the objective of the present study to analyse angles between cracks for a variety of different soils and drying conditions.

THEORY

In order to quantify different patterns of cracks which are observed under field conditions a basic principle is necessary. This is provided by the assumption that the tensile stresses which cause the cracking originate from contraction of water menisci. The lines of failure, however, and thus forms of aggregates which are developed between them are governed by external factors. The most prominent of these is the geometry of the matrix in which

the tension field developes. A finegrained sediment will start cracking at the location where tensile stress surpasses tensile strength first. Under field conditions this usually will be at the surface of the sediment. On such a more or less horizontal plane under these conditions there are two occasions for the start of the initial crack:

1) Concentration of strain in limited areas, caused by gradients of strain as a consequence of incomplete redistribution of water in neighbouring areas or by change of texture.

2) Concentration of contractive stress at places where the sediment is the shallowest.

In both cases cracks provide relaxation of tensile stresses. Since maximum stresses will concentrate at the tips of cracks [4], the maximum relaxation will be obtained the easiest by increasing the length of an existing crack. Linear growth or change of direction, however, will depend on the local conditions (1) and (2).

As soon as stresses develop in the matrix again, after relaxion by cracking, at both sides of the primary crack, a new generation of cracks develops. These can initiate analogously to the previous one somewhere in the matrix. At the walls of the primary crack enhanced evaporation creates additional stress, Therefore the most effective relaxation is likely to occur in orthogonal direction to the crack first formed. Further growth of the cracks of both generations will be governed by the same conditions as already described. In the same way a tertiary generation of cracks will develop and so on.

Because tensile failure occurs in all these cases, in a homogenous isotropic sediment orthogonal angles (OA) should form between cracks of different generations. A crack that comes by growing close to an already existing older one, will turn towards it so that again right angles are formed at the junction. This would provide macroscopically maximal relaxation of the isotropic stress originating from microscopically contracting menisci.

Besides tensile stress shearing stress is the other mechanism that can cause failure. It is created by contracting menisci too. Unlike tensile failure it will produce combinations of cracks that do not meet rectangularly. They will be mostly combinations of non orthogonal angles (NOA) that oscillate either around 45° or around 135° because of the influence of the internal friction at the moment of cracking. The two groups of deviations from rectangularity should always be noticeable in these cases. The mean values of both groups should add to give 180° in the same way as for the two rectangular angles. The relations of these both patterns of cracks are shown in Fig. 1. The relation of the developing angle of failure α (°) to the internal friction φ (°) is given by the formula from classical soil mechanics [9]:

$$\alpha = 45° \pm \varphi / 2 .$$

In this paper results of investigations on the relation of these both groups of angles in the primarily shrinking finegrained soil material are given.
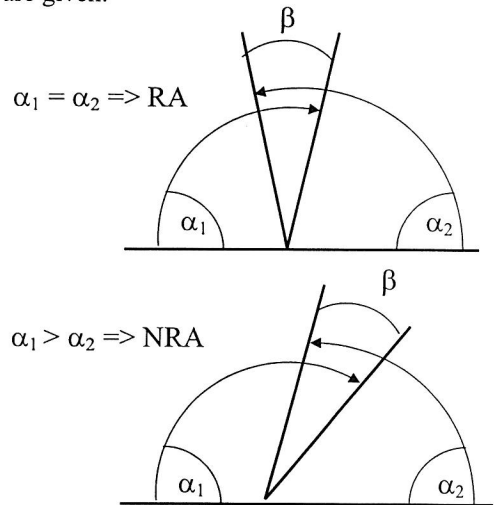

Fig. 1. Scheme of combinations of angles caused by tensile failure (above) and by shear failure (bottom) α = measured angles, β = deviation caused by local conditions.

MATERIAL AND METHODS

Measurements of angles between two interconnected cracks were performed at two groups of materials. The photographs of (Figs 2-4) show in situ situations:
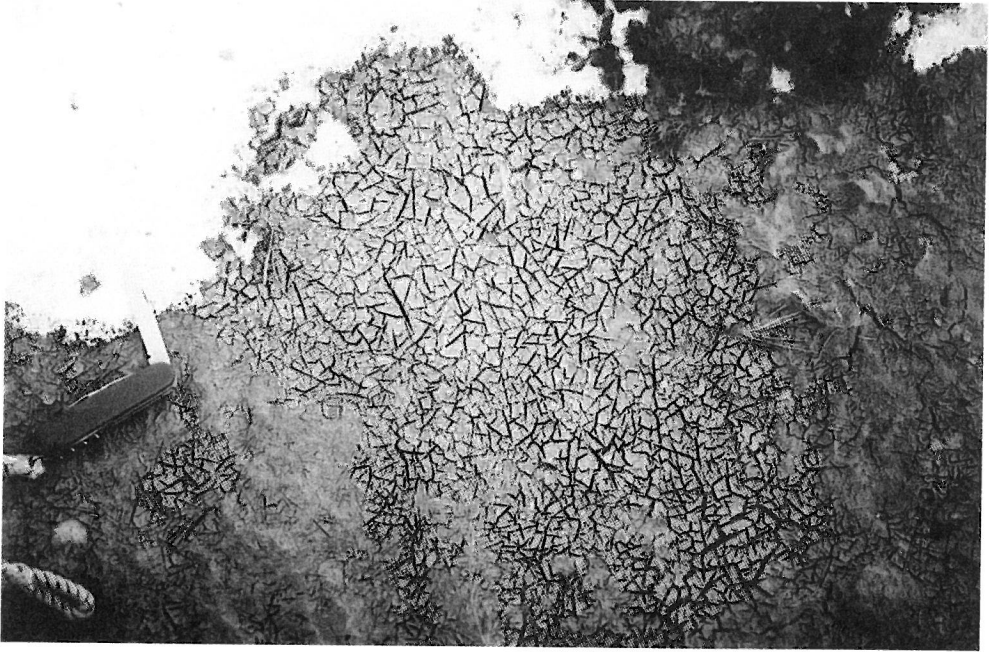
Fig. 2. Cracks developed in fresh silty tidal sediment after freezing at low tide. Tidal flat, Eiderstedt, Schleswig-Holstein (A).
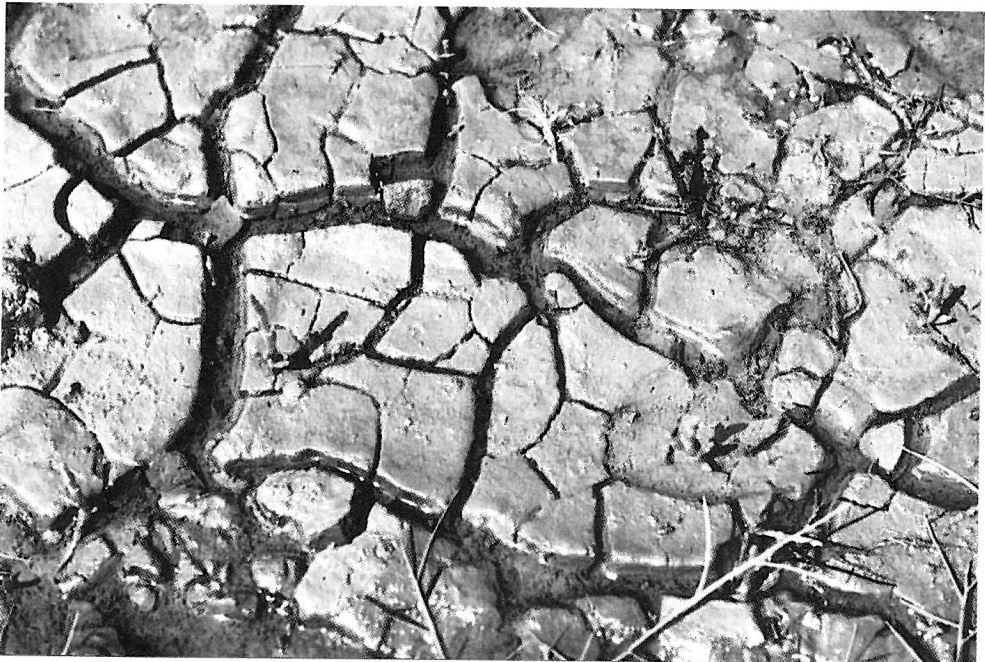

Fig. 3. Cracks developed in fresh tidal sediment after drying at low tide. Ditch at tideway, Eiderstedt, Schleswig-Holstein (B).
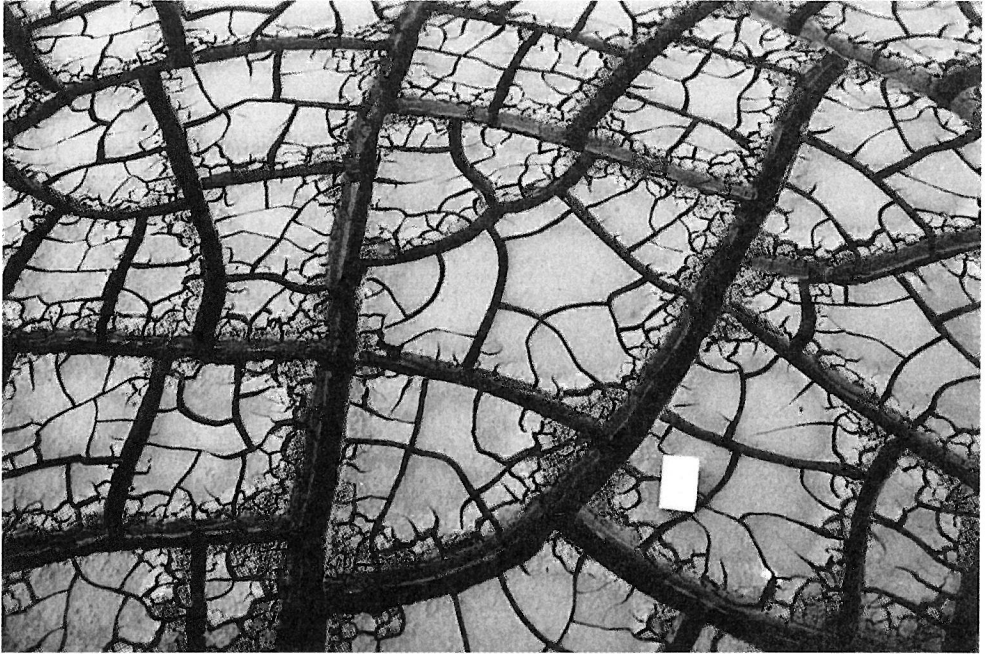
Fig. 4. Cracks developed in silty colluvium from weathering residue from limerock after drying Capernaum, Israel (Photograph Dr.B.Beyme, Hannover April 1981) (C).

1) Fresh tidal sediments formed at the shore of the North Sea (German Bight):

Sample A (Fig. 2) frozen after recess of the tidal water.

Sample B (Fig. 3) air dried after recess of tidal water.

Sample C (Fig. 4) colluvium from noncalcarious weathering residue accumulated after a heavy rainfall near Capernaum, Israel.

In all three cases the material is composed mainly of silt, containing some clay but only neglectable amount of sand. The original size of the objects is about 40x40 cm for Fig. 2 and 70x 80 cm for Figs 3 and 4.

2) Additionally, photographs of laboratory experiments were analysed from literature [5,10]. In contrast to the former group, the laboratory experiments were performed under reproducible conditions. We analysed:

Figure 2 from [5]. 20 g aggregates < 2mm mixed and molded with 20 cm^3 deionized water to give a 25 mm thick layer in 9x9 cm boxes.

Regosol with 48% clay and Fluvisol with 46 % clay.

Figure 3 from [10]. Uri-Bentonite, prepared in the same way as the former.

Measurements were performed on photographs (group 1) and xerocopies (group 2) magnified to a size of 21x29 cm (DIN A4). A set-square-goniometer from acrylic glass with a basis length of 20 cm was used combined with a movable lever made from 0.5 mm acrylic glass.

At each of the 6 objects at least 70 angles were measured. The accuracy of reading from the instrument was 0.5°. The accuracy at the objects was limited by the blurred crack-edges of the magnifications. In order to determine this accuracy, situations were selected, where three cracks originated at one point. Adding the three angles from 9 such domains for the Uri-Bentonite [10] resulted in a mean of $359 \pm 6.49°$. Thus a standard deviation of 2 - 4° was assumed for an individual angle.

RESULTS

Results obtained from the Uri-Bentonite-slurry of [10] corresponded best to the hypothesis of rectangularity between tensile stress cracks. Orthogonal angles (OA) were obtained in 84% of all the measurments. In spite of the calculation of standard deviation mentioned above, it rather arbitrary, how the sector of right angles should be defined. Therefore in Table 1 statistical parameters are given for sectors of 90 ±1° until 90 ± 9°. It is evident that standard deviation of the means of OA increases with increasing width of the sector. In order to quantify statistically the form of the distribution, median and quartiles were computed. It can be seen that the sum of Q1 and Q3 is always close to 180°, regardless of how the sector is chosen. So there is no obliquity. The continuous decrease of the difference between Q1 and Q3 if the sector of OA is decreased, does not give any hint as to the irregularity of the distribution, i.e., the occurrence of non orthogonal angles (NOA) within this group.

There were 11 angles, which deviated by 10° and more, from rectangularity. If these were considered to be non orthogonal angles (ORA), i.e., formed by shearing cracks, then the sum of their means should be close to 180° as well. This hints towards the existence of shearing cracks in this material with angles which deviate up to 40° from rectangularity (Fig. 5). Arithmetic means for these angles were calculated separately for those <80 and >100° and included into Table 1.

Data from the other 5 materials were analysed analogously to those of the Uri-Bentonite. Again, all means were close to 90° as with the Bentonite in the Table 1, regardless of how the sector for OA was defined. Therefore only standard deviations are given in Table 2. The same sectors for rectangularity were used as in Table 1, merely one wider sector was added. Again no abrupt change in standard deviation can be observed if the sector for rectangularity is increased. Of course, this increase is paralleled with an increase of percentage of OA (Table 3). From Table 3 it can be seen further that the percentage of OA in the laboratory experiments is more similar to that observed in the open air drying patterns compared to a frozen sample.

Even with the widest sector allowed for rectangularity (78 - 102°) there are always some angles beyond that limit. This fact indicates that shearing cracks exist always in the patterns. Their amount is the highest in the frozen sample (Fig. 2). For these angles mean values and standard deviations were calculated separately for the sectors <80 and >100°. They are given in Table 4 together with the sum of their means.

T a b l e 1. Statistical parameters of the angles between cracks in the dried slurry of Uri-Bentonite for differently wide sectors defined for orthogonal angles OA (top) and non orthogonal angles NOA (bottom) (Values from Fig. 3, [10]). Arithmetic means, medians, quartiles, their sums and their differences

Orthogonal angles (OA) sector (°)	Number of readings	$x \pm s$	Median	Q_1	Q_3	Q_1+Q_3	Q_3-Q_1
81 - 99	57	90.4 ± 2.20	90	89	92	181	3
83 - 97	55	90.4 ± 2.80	90	89	92	181	3
86 - 94	45	90.1 ± 1.80	90	89	91	180	3
88 - 92	37	90.0 ± 1.25	90	89	91	180	2
89 - 91	25	90.0 ± 0.68	90	90	91	181	1
Non orthog. angles (NOA)							
<80°	6	71.1 ± 8.30					
>100°	5	110.4 ± 8.30				sum = 181.5°	

T a b l e 2. Standard deviations of the means of orthogonal angles (OA) calculated for different sectors. Laborarory soils: Uri = Bentonite (values from Fig. 3 [10]), Rego = Regosol, Fluvi = Fluvisol (values from Fig. 2 [5]). In situ systems: A = tidal flat cracks after freezing, B = tidal flat, cracks after partial drying, C = Collivium, Israel, cracks after severe drying

Sample	Sector (°)					
	78 - 102	81- 99	84- 96	86 - 94	88 - 92	89 - 91
Laboratory						
Uri		3.22	2.8	1.8	1.25	0.68
Rego			2.7	1.7	0.91	0.63
Fluvi		4.21	3.38	2.0	0.90	0.33
in situ						
A (frozen)	6.0	4.1	2.7	2.58	1.74	<0.05
B	5.5		2.0	1.92	0.18	0.18
C (arid)	4.82		2.25	1.92	1.05	0.58
x			2.63	1.98	1.00	0.41

T a b l e 3. Proportion of orthogonal angles (OA) as a percentage of the total number of values for different width of the sector of rectangularity. Names of samples see Table 2

Sample name	Total number of readings	Ranges defined for right angles (°)				
		78 - 102	81 - 99	84 - 96	88 - 92	89 - 91
Lab.samples						
Uri	68	86	83	79	56	38
Fluvi	113	55	54	38	20	16
Rego	102	58	53	49	32	29
in situ						
A (frozen)	164	16	13	5	5	0.6
B	108	51	42	39	27	27
C (arid)	152	71	66	49	39	31

T a b l e 4. Non orthogonal angles (NOA) < 80 and > 100°. Arithmetic means, standard deviations and sum of the means. Angles of internal friction AIF (φ) calculated from the means

Sample name	Angles < 80°	Angles > 100°	Sum a+b	φ (a)	φ (b)
Lab.samples	(a)	(b)			
Uri	71.1 ± 8.1	110.4 ± 2.0	181.6	52.2	49.2
Fluvi	67.8 ± 6.4	115.4 ± 10.0	183.3	45.6	39.2
Rego	69.4 ± 7.1	112.9 ± 7.6	182.4	48.8	44.2
in situ					
A (frozen)	59.6 ± 13.3	122.2 ± 11.6	181.8	29.2	25.6
B	63.6 ± 12.1	114.4 ± 12.2	178.0	37.2	41.2
C (arid)	70.3 ± 5.8	108.7 ± 6.2	179.1	50.6	52.6

This sum is in all cases almost 180°. This fact indicates that both these groups developed at the same internal friction of the material. The angles of internal friction (AIF) were calculated for both of these groups using equation (Table 4). The AIF calculated from the group of values greater than OA and those from the group smaller than OA agree the better, the closer the sum of their means approaches 180°.

The definition for NOA for the sector <80 and >100° is primarily arbitrary. The limits were positioned to avoid as securely as possible that OA, i.e., tensile cracks are counted as NOA.

In order to test the validity of this assumption the AIF were recalculated including the values closer to the sector of OA. These angles are given in Table 5 together with the limiting value for each individual sample in the last column (e and f in Table 5). The values of the narrower (a and b) sector of NOA are highly correlated to those calculated for the wider sector (c and d) (r = 0.9406, p<0.5%). This result does not show improvement in the delimitation of OA against NOA. Even if these somewhat uneven distributions are used, the sum of the readings is close to 180° (Table 5, value at bottom of column e/f).

T a b l e 5. Angles of internal friction AIF (φ) calculated from means of non orthogonal angles NOA (a and b, see also Table 4) compared with the means calculated from wider sectors of NOA (column c and d) and their limiting highest angle $\alpha1$ (e) and the lowest angle $\alpha2$ (f) for each of these sectors. (Notation $\alpha1$, $\alpha2$ see Fig. 1)

Sector	φ (<80°) (a)	φ ($\alpha < 1$) (c)	Values (°) (e)
Lab. samples			
Uri	52.2	52.2	80
Fluvi	45.6	52.0	87
Rego	48.8	52.0	82
in situ			
A (frozen)	29.2	32.0	83
B	37.2	46.0	86
C (arid)	50.6	60.0	85
Arithm.mean (x)	43.9	49.0	83.8 (=90 - 6.2)

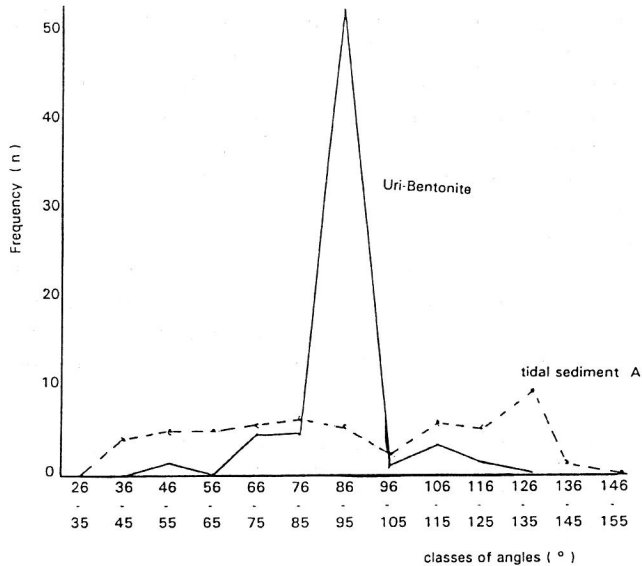| Sector	φ (>100°) (b)	φ (> $\alpha2$) (d)	values (°) (f)
Lab. samples			
Uri	49.2	49.2	100
Fluvi	39.2	43.8	93
Rego	44.2	46.2	97
in situ	25.6	28.0	97
A (Frost)	41.6	46.0	97
B	52.6	62.0	95
C (arid)			
Arithm.mean(x)	42.0	45.8	96.5 (=90 + 6.5)
total sum of the means of non orthogonal angles NOA		180.3°	

Fig. 5. Frequency distributions of angles between two cracks subdivided into classes of 10° each, from Uri-Bentonite ([10] all measured values) and from tidal sediment after freezing (A) (every third from a file of values ranked from 35 through 146°). The class 86-95° includes the orthogonal angles if the middle range of these angles is taken from line 3 in Table 1.

The very narrow distribution of the angles in the Uri-Bentonite causes, that for this sample the figures in Table 5 in columns (a and c) and (b and d) for this material are equal. The distribution of angles of the two most different samples are depicted in Fig. 5.

CONCLUSIONS

The results show that at primary shrinkage - which in essence is normal-shrinkage [6] - cracks develop. They are caused by tensile stress and meet at right angles. But at the same time in all the samples cracks were observed, which points to simultaneous development of shear stresses. Every individual angle must fit into one of these two classes. But finding limits between these two groups is difficult because heterogeneity of material, depth of the soil shrinking to deeper layers and quality of contact will effect the geometry of crack promotion. If the arbitrarily defined sector of NOA is enlarged, i.e., the tolerance of deviation for the OA is reduced, the calculated AIF increase. Table 5 shows an example for the case that the sector for OA as given in Table 4 (80 - 100 °) is

diminished up to 7°. This applies to both groups of readings (<90 and >90°) to an almost identical extent. It is concluded that NOA always exist, regardless how the sector of OA is defined. That means that there is always cracking caused by shear stress. The angles of internal friction in Table 5 show that cracking caused by shear stress occurred at a comparatively soft and consequently wet situation with a frozen sample (Fig. 2). Cracking in the soil from the arid area (Fig. 4) should have developed at a condition of high internal friction, i.e., at a drier state. The distributions of values from the laboratory sample Uri-Bentonite (16% NOA) and from the frozen in situ sample (A) with 10% OA which are depicted in Fig. 5 are extreme situations concerning the relative occurrence of OA and NOA. All the rest of the samples show intermediate conditions.

The results of the calculated AIF aggree well with earlier findings [7]. It may be concluded therefore that the proportion between OA and NOA can be used to distinguish patterns of cracks in soils. Calculated angles of internal friction might give information on the local drying process and cracking conditions.

REFERENCES

1. **Barzegar A.R., Rengasamy P., Oades J.M.:** Effects of clay type and rate of wetting on the mellowing of compacted soils. Geoderma 68, 39-49,1995.
2. **Chertkov V.Y.:** Evaluation of soil crack net connectedness and critical stress-intensity factor. Int. Agrophysics, 9, 189-195, 1995.
3. **Dexter A.:** Two types of anisotropy induced by the passage of a wetting front. Soil Sci. Soc. Am. J., 47, 1060-1061, 1983.
4. **Griffith A.A.:** The phenomena of rupture and flow in solids. Phil. Trans. Roy. Soc. London., Vol. VL, 219-230, 1921.
5. **Guidi G., Pagliai M., Petruzelli C.:** Quantitative size evaluations of cracks and clods in artificially dried soil samples. Geoderma, 19, 105-113, 1978.
6. **Hartge K.H.:** Vergleich der Schrumpfung ungestörter Böden und gekneteter Pasten. Wissenschaftl. Z. Fr.-Schiller-Universität Jena. Mathem.-Naturw. Reihe 14, Heft 3, 53-57, 1965.
7. **Hartge K.H.:** Der Scherwiderstand von Bodenaggregaten. Trans. X. Int. Congr. Soil Sci., Moscow, 1, 194-202, 1974.
8. **Hartge K.H., Bachmann J.:** Morphologic analysis of soil aggregates using Euler's polyeder formula. Soil Sci. Soc. Am. J., 63, 930-933, 1999.
9. **Lang H.-J., Huder J.:** Bodenmechanik und Grundbau. Springer Berlin, Heidelberg, New York, 1982.
10. **Pertuzelli G., Guidi G., Sequi P.:** Electrooptical measurement of clay shrinkage. Clay Min., 11, 81-84, 1976.
11. **Preston S., Griffiths B.S., Young I.M.:** An investigation into sources of soil crack heterogeneity using fractal geometry. Europ. J. Soil Sci., 48, 31-37, 1997.
12. **Puentes R., Wilding L.:** Structural restoration in Vertisols under pasture in Texas. Trans. 14. Int. Congr. I.S.S.S., Kyoto, 7, 244-249, 1990.
13. **Vallejo L.E.:** The brittle and ductile behavior of clay samples containing a crack under mixed mode loading. Theoretical and Applied Fracture Mechanics, 10, 73-78, 1988.